Polyethylene/Boron Nitride Composites for Space Radiation Shielding

Courtney Harrison,[1] Sean Weaver,[2] Craig Bertelsen,[2] Eric Burgett,[3] Nolan Hertel,[3] Eric Grulke[1]

[1]*Department of Chemical and Materials Engineering, University of Kentucky, Lexington, Kentucky 40506*
[2]*Lexmark International, Inc., Lexington, Kentucky 40505*
[3]*Nuclear and Radiological Engineering, School of Mechanical Engineering, Georgia Institute of Technology, Atlanta, Georgia 30332*

Received 26 June 2007; accepted 11 December 2007
DOI 10.1002/app.27949
Published online 9 May 2008 in Wiley InterScience (www.interscience.wiley.com).

ABSTRACT: Composites made with boron might be absorbers of low energy neutrons, and could be used for structural materials for spacecraft. Polyethylene/boron nitride composites were fabricated using conventional polymer processing techniques, and were evaluated for mechanical and radiation shielding properties. The boron nitride powder surfaces were also functionalized to improve interfacial adhesion. Addition of neat boron nitride to an injection molding grade HDPE increased the tensile modulus from 588 to 735 MPa with 15 vol % filler. The bonding of a trifunctional alkoxysilane to the powder surface prior to processing increases the composite modulus to 856 MPa at the same loading. Scanning electron microscopy of fracture surfaces verified that the silane-treated powders had improved adhesion at the filler/polymer interface. Radiation shielding measurements of a 2 wt % boron nitride composite were improved over those of the neat polyethylene. © 2008 Wiley Periodicals, Inc. J Appl Polym Sci 109: 2529–2538, 2008

Key words: polyethylene; boron nitride; composites; space radiation shielding

INTRODUCTION

Space radiation shielding has been an important element of manned space flight for some time, including near-earth missions such as the International Space Station.[1] Interplanetary travel will take astronauts outside of the van Allen belts and into an increased radiation environment that includes galactic cosmic rays (GCRs) and solar energetic particle (SPE) events. Early studies of missions to Mars considered the radiological tolerance criteria for spacecraft,[2] which are still being debated.[3] Protection strategies such as habitat shields and radiation ''storm'' shelters[4,5] are complex because the shielding materials need to be integrated into the spacecraft or habitat design criteria.

In-transit protection strategies are different for GCRs and solar particle events. Solar energetic particles mostly consist of low energy protons,[6] and additional shielding material is likely to be the preferred solution. GCRs are ions of the elements between hydrogen and nickel, with broad energy spectra between 10 MeV to millions of MeV.[7] Biological data on mammalian exposures suggest that the conventional shielding material, aluminum, will permit increases in cancer induction rates even for relatively thick shield sections. Materials with high hydrogen contents can fragment GCR to less damaging particles. Those with low atomic number may produce low numbers of secondary particles and, in particular, fewer neutrons that lead to biological damage.[8] Recent studies have proven Wilson's et al. theory that the effectiveness of the shield is directly related to mass number. As the mass number decreases the performance is enhanced, in particular with hydrogen being the best material.[9]

Polymer composite shielding material concepts

The shielding properties of the structural components are just as important as those from dedicated shielding materials and must be considered in design of future spacecraft.[9] Multifunctional polymer composites incorporating inorganic additives could potentially provide structural, radiation shielding, and even flame retardancy properties. There are many ways in which polymer composites can be used for space radiation shielding applications, e.g., one already being investigated is polymer binders for local regolith for exterior habitat walls. NASA has focused on shielding properties of polyethylene because of its high hydrogen content, and has chosen it as the reference material for current multifunctional composites being developed.[10]

Correspondence to: E. Grulke (egrulke@engr.uky.edu).
Contract grant sponsor: NASA; contract grant number: NNM04AA60G.

There is prior literature on polymer composites developed specifically for radiation shielding applications. Low-density polyethylene, chosen for its radiation shielding properties, has been paired with hollow glass spheres which improve the modulus with a minimum weight gain.[11] Poly(4-methyl-1-pentene) is similar to polyethylene with respect to high hydrogen content. It has been paired with carbon nanotubes for improved modulus.[12] Polystyrene has slightly lower hydrogen content and has been paired with lead dimethacrylate, which can incorporate lead atoms directly into the polymer chains,[13] and with lead oxide particles.[14] Epoxy paired with graphitic nanofibers has a very high modulus compared to polyethylene composites, but the radiation shielding is not quite as good.[15] Elastomeric composites have been developed using natural rubber with gadolinium acrylate to incorporate the shielding element into the polymer chain.[16] High-strength polyimides have been paired with boron-rich powders and whiskers.[17,18]

Space radiation shielding polymer composites based on commercial polyethylenes would have processing advantages, and could be easily fabricated into sheets for laminates, extruded into profiles or foams, and injection-molded for structural parts. Fillers such as boron-rich additives could improve the shielding characteristics as well as improve the modulus. This work is based on commercial polyethylene resin with an inorganic boron-rich additive, boron nitride (BN). These composites should also be advantageous because of their lighter weight with increased shielding properties.

Effects of fillers on composite mechanical properties

An important challenge for developing polymer composites is creating good adhesion between the polymer phase and the inorganic filler. Polyethylene has hydrophobic surfaces (its water contact angle is $\sim 90^\circ$) and a critical surface tension of 33 dynes/cm. Therefore, fillers with polar surfaces, such as boron nitride, will tend to have poor adhesion to the polymer and can act as nonreinforcing fillers, lowering the mechanical properties of the composite.

Low levels of BN, 0.1–0.5%, are added to polyethylene extrusions to suppress melt fracture and sharkskin effects while retaining mechanical properties. Two mechanisms contribute to these effects. The first is thought to be migration of the hexagonal boron nitride platelets to the die walls, where slippage of the melt at the wall is induced.[19] The second mechanism is the sorption of polyethylene chain segments on boron nitride surfaces.[20,21] The sorbed chains are thought to decrease extensional stresses responsible for melt fracture by dissipating the release of energy from isolated rupture of the melt.[22] Boron nitrides with different surface energies induce different melt fraction behavior.[23,24]

Rigid fillers, such as calcium carbonate, can be used to increase the modulus and yield stress of HDPE.[25] Good adhesion between the rigid filler particles and the polyethylene continuous phase help to improve the matrix ligament thickness during fracture, increasing the matrix toughness.[26–30] Both stearic acid[26,30] and silanes[31] have been used to improve the adhesion between fillers and HDPE.

Boron filler functionalization

Functionalization of filler particles is often used to improve adhesion between the filler and the polymer matrix. Trifunctional alkoxysilanes are widely available and can react with surface hydroxyl groups on inorganic fillers. Surface analysis of boron nitride powders by FTIR[32] has confirmed the presence of hydroxyl and acidic oxygenated sites.

This work focuses on increasing the mechanical properties of boron-rich composites over that of neat polyethylene. Boron nitride composites were fabricated using conventional polymer processing methods, and evaluated for mechanical and radiation shielding performance. Surface functionalization was used to improve the adhesion between boron nitride and polyethylene. Currently, the most common use for a boron nitride/polyethylene composite is in the electronics industry because of its thermal conductivity characteristics[33]. These applications have focused on larger amounts of filler than we have developed, but mechanical and morphological properties of the composites will be identified.

EXPERIMENTAL

Materials

High-density polyethylene was used as purchased from Dow Chemical Company (Houston, TX) grade NT 8007. This injection molding grade would be appropriate for structural elements of the spacecraft. The boron nitride, supplied by GE Advanced Ceramics (Cleveland, OH). Grade HCP was used as received with a mean particle size of 7–10 μm. The platelet morphology of the particles is shown in Figure 1. Silane coupling agents were purchased from Gelest (Morrisville, PA).

Tensile specimen testing

Composites were made by mixing polyethylene with solids in a Haake Rheomix (Waltham, MA) melt blender (145°C, 30 min). The polymer was initially allowed to melt in the blender at temperature, and the powder samples were slowly added to the molten material with mixing. The material was then

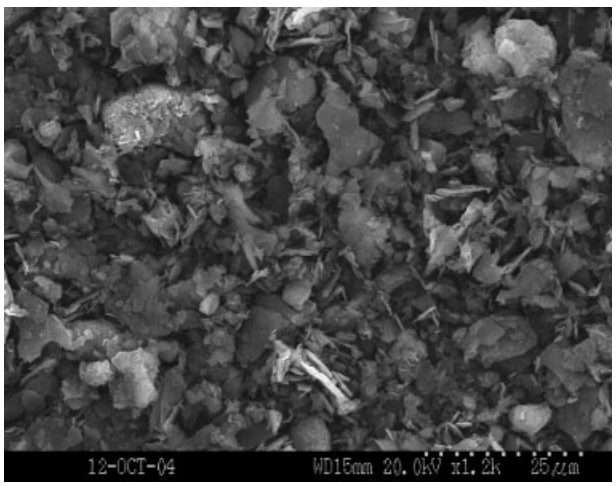

Figure 1 SEM micrographs of boron nitride particles showing platelet structure.

removed from the blender, cooled and crushed using a hammermill crusher (> 0.5 mm). Crushed material was placed in a thin film mold and compressed at 150°C for 15 min using a Carver Lab Press Model C (Wabash, IN). The films were 0.002" in thickness. Dogbone samples were cut using an ASTM D 638 Type IV Die. The mechanical properties were determined on dog bone samples using a MTS QTest 10 (Eden Prairie, MN) with a strain rate of 0.0167 s^{-1} and repeated five times. The average standard error for tensile modulus was 55.1 MPa. The strain at break values are reported with a standard error of 34.5%, and tensile strength has an average standard error of 1.5 MPa.

FTIR spectra

FTIR spectra were taken with a Nicolet MagnaIR 560 spectrometer using a Thunderdome Smart accessory with a germanium window for powder samples.

Filler functionalization

Powder samples were functionalized to improve adhesion between the powder and continuous phase. Trifunctional alkoxysilane coupling agents were dispersed in water for several minutes at 60–70°C. The boron nitride was then added to the solution and allowed to mix for 20 min. The samples were filtered, washed, and dried in an oven for 12 h at 110°C. The coupling agents used are shown in Table I.

Neutron and proton attenuation measurements

For neutron attenuation purposes, the material was pressed into solid plaques. These plaques were ~ 11.25 cm × 7.95 cm × 0.5 cm thick. These samples were tested against aluminum, which is a conventional, standard material used for space radiation shielding. The samples were tested at both the Los Alamos Neutron Science Center (LANSCE) Weapons Neutron Research (WNR) neutron facility as well as the Fermi National Accelerator Lab (FNAL). At LANSCE, the samples were tested in the WNR beam on the 30 left flight path (FP30L). The neutron beam at FP30L was selected for neutron testing because it delivers up to 600 MeV neutrons, whose energy spectra can be seen in Figure 2. The measured spectrum is taken from time of flight data. Below 1.5 MeV, there is insufficient time to process time of flight data. The samples were tested in the unfiltered beam and error bars are smaller than the symbols.[34] The neutrons are produced by spallation events caused by an 800 MeV pulsed proton beam incident on a tungsten target. These spallation neutrons have a very similar energy spectrum to that of neutrons at 40,000 feet, an area of interest for high altitude flight and low earth orbit. At FNAL, the M02 beam line was used to deliver 120 GeV protons to measure attenuation. 120 GeV protons were selected because of their ease of extraction from the Main Injector, and because their energy level is near the maximum energy flux of GCR. Figure 3 shows the GCR energy flux as a function of nucleon energy that has been measured in near earth orbit, which shows the ''knee'' in the cosmic ray spectrum for H nucleons. The 120 GeV protons are right above the theoretical ''knee'' in the GCR spectrum. Figure 4 shows that particles with energies of 120 GeV nucleons are not attenuated by the magnetic shield near the earth and constitute a significant radiation hazard.

A 30 cm × 30 cm × 30 cm tank phantom was used to measure the shielding effectiveness. Absorbed dose measurements were made at various depths with several different thicknesses of shielding material and aluminum (1100 grade) to determine the relative shielding effectiveness. If polyethylene-based composites can perform as well or better than the aluminum, than the polyethylene compounds are a superior choice. Polyethylene compounds, comprised of only light nuclei, have a much lower neutron yield in high energy particle reactions. Figure 5 shows the radiation dose rates as a function of thickness when aluminum is used as a shielding material. The incoming flux of GCRs interacts with aluminum, forming secondary protons and neutrons (cascade particles). These cascade particles actually increase the local dose rate as the distance through the shielding material increases. As the cascade particles are absorbed in turn, the total dose rate then goes through a maximum and then decreases. With a lower Z number, polyethylene will provide a lower secondary radiation field by decreasing the secondary dose from protons and neutrons.[36]

TABLE I
Trimethoxysilane Coupling Agents

Common name	CAS Reg. No.	Symbol	Structure
Styrylethyl trimethoxysilane	134000-44-5	C	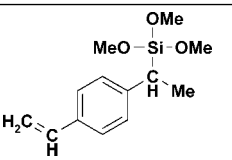
Vinyl trimethoxysilane	2768-02-7	D	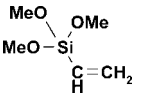
Methacryloxypropyl trimethoxysilane	2530-85-0	E	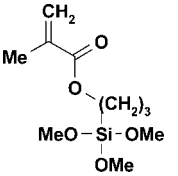
[Methoxy(polyethyleneoxy) propyl] trimethoxysilane	65994-07-2	F	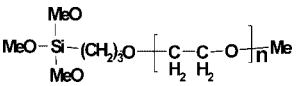
β-Glycidyloxyethyl trimethoxysilane	20526-39-0	G	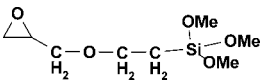
n-Octadecyl trimethoxysilane	3069-42-6	H	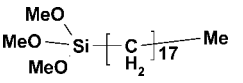

In addition, aluminum can become activated or produce long-lived spallation products that the lighter atomic composition polyethylene compounds do not. These spallation and activation products can build up over long exposure periods and contribute additional dose to the payload it is shielding. A tis-

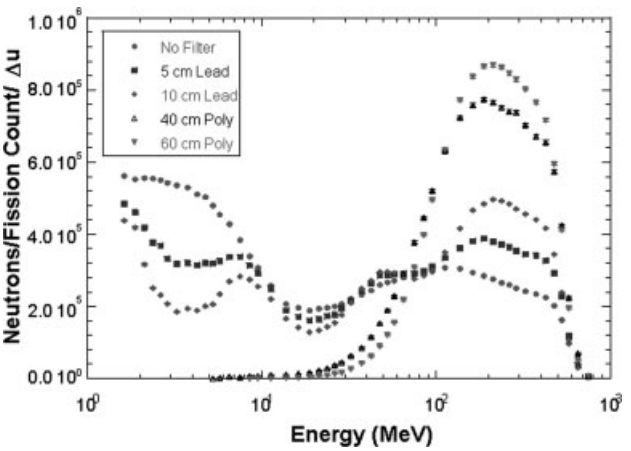

Figure 2 Measured neutron spectrum at the LANSCE WNR FP30L beam.[34]

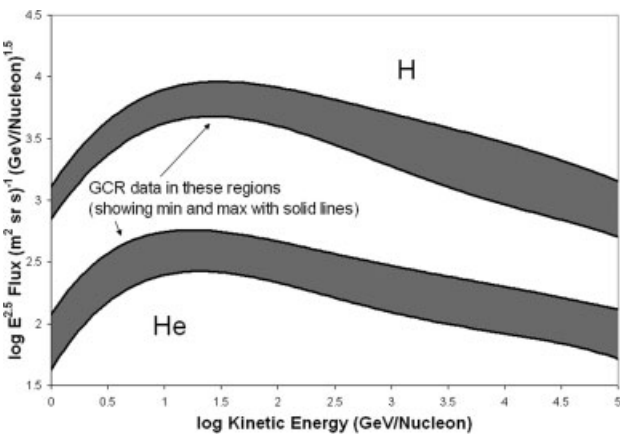

Figure 3 Cosmic ray experimental spectra from the JACEE 1–12 measurements in a near earth orbit.[35]

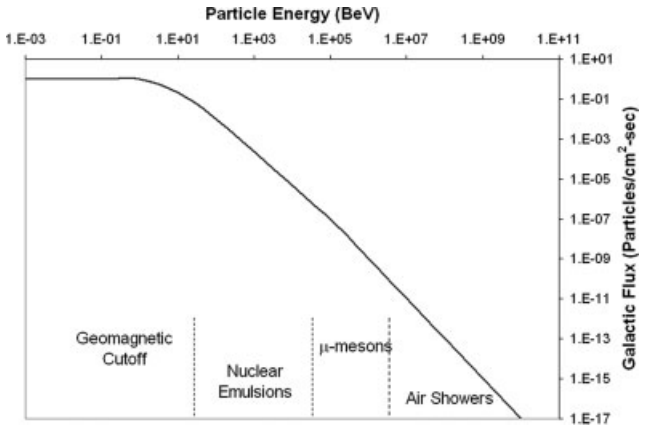

Figure 4 The overall galactic cosmic ray energy spectrum.[36]

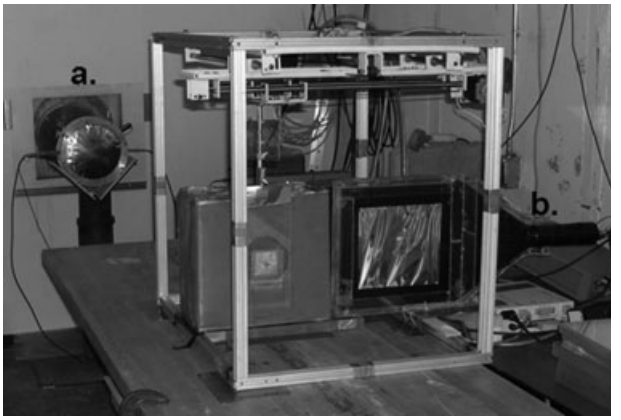

Figure 6 Neutron detectors (a: WNR fission chamber; b: ''Banjo'' detector) used in experiment.

sue-equivalent ion chamber made out of A150 tissue-equivalent plastic was used to measure the absorbed dose in the tank. This integral measurement of dose allows a direct measure of shielding effectiveness. Because of the fluctuations of these beams, beam monitors were used to normalize the results. The setups for the LANSCE measurement and FNAL measurements can be seen in Figures 6 and 7.

RESULTS AND DISCUSSION

FTIR characterization of functionalized boron nitride

All the coupling agents selected (Table I) have the same trimethoxysilane functional group for reaction with the surface, and differ by the functional group attached to the trimethoxysilane. Silanes C, D, and E contain C=C bonds and could homopolymerize by thermal initiation or free radical initiation, might be susceptible to polymerization with residual catalyst in the polyethylene, or could polymerize with free radicals generated at defect sites on polyethylene chains at higher temperatures. The vinyl trimethoxysilane has a short spacing between the surface and its functional group, while the styrylethyl and methacryloxypropyl functional groups provide increasing distance between the surface and the functional group. The methacryloxypropyl functional group is polar, and the other two reactive silanes are nonpolar. The next three silanes have longer chain segments: a polyethylene oxide oligomer, a reactive epoxy, and an alkane.

Figure 8 shows the FTIR spectra for BN powders treated with coupling agent F compared to the spectrum for the untreated powder. The silanized powder shows a broad OH peak present between 3100 and 3600 cm^{-1} and also a small peak near $\sim$ 1750 cm^{-1} that could be due to water. A small spike is also seen just below 3000 cm^{-1} from the aliphatic $—CH_2—$ and $—CH_3$ groups. Silane groups are detected by the absorption peaks between 1000 and

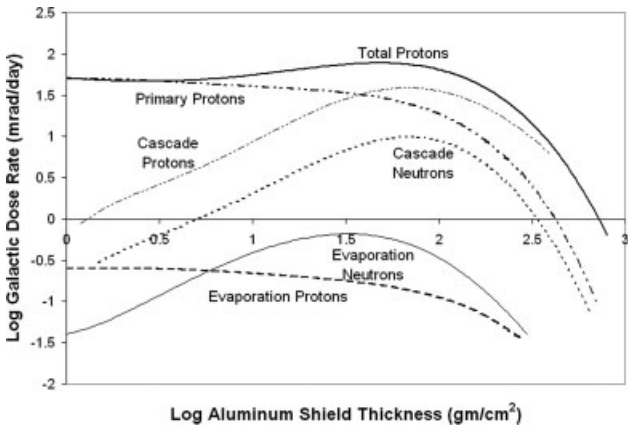

Figure 5 Radiation dose rates as a function of shield thickness of aluminum.[36]

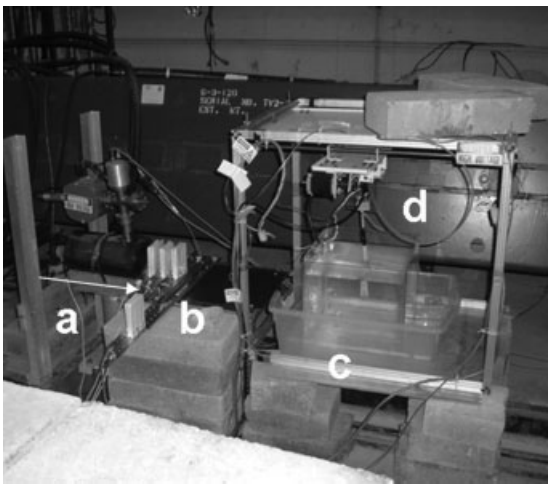

Figure 7 Fermilab shielding experiment setup with ion chamber (shown as d) Submerged in water phantom (shown as c) with (a) representing the beam and (b) shielding samples.

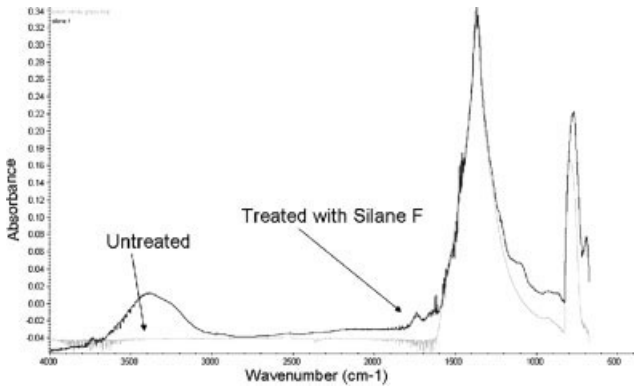

Figure 8 FTIR spectra for boron nitride particles with silane coupling agents.

1200 cm^{-1} indicating Si—O bonds. The other five silanized powders also showed evidence of chemical coupling between the silane and the BN surface.

Mechanical properties of composites

Thin film tensile tests were performed for HDPE with neat boron nitride powder and silanized boron nitride powders to determine how surface modifiers affected tensile strength, toughness, and Young's modulus.

Elongation at break/toughness

Figure 9 shows averaged stress–strain curves for five replicates of HDPE and six different volume % BN fillers. This particular HDPE has an elongation at break of $\sim$ 300%. Nonreinforcing fillers often greatly reduce elongation at break as the particles act as defect sites that initiate failure in the continuous polymer phase. One volume percent boron nitride filler reduced the elongation at break to $\sim$ 85%, with larger volume fractions resulting in lower elongations at break.

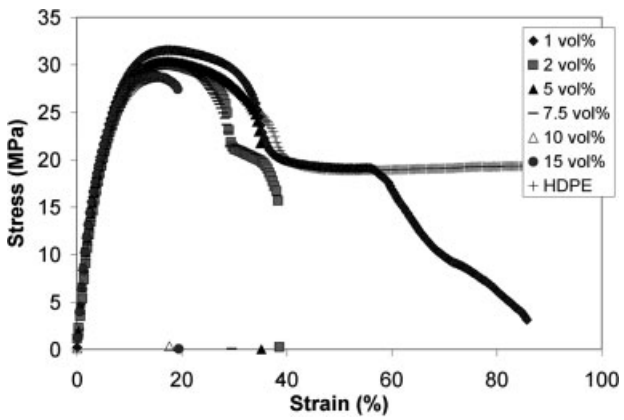

Figure 9 Stress versus strain curve for HDPE and untreated boron nitride focusing on low strain rates.

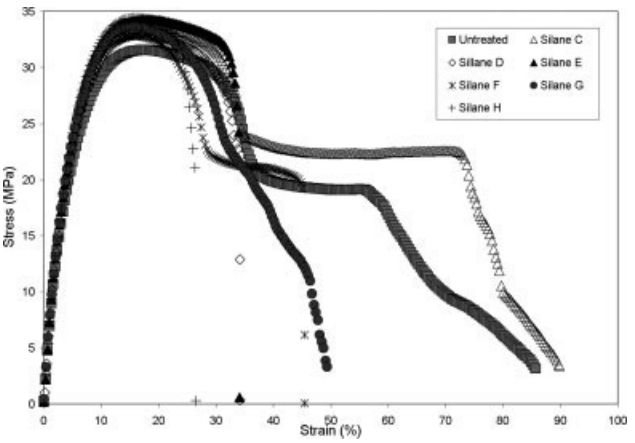

Figure 10 Stress versus strain curve for untreated boron nitride and boron nitride treated with different silane coupling agents present at 1 vol % in HDPE.

Figure 10 shows the stress versus strain curve for silanized boron nitride particles at 1 vol % in HDPE. Only one silane coupling agent, styrylethyl trimethoxysilane, produced a composite with a similar elongation at break to the neat boron nitride filler. This coupling agent has a styrene group in the backbone and a vinyl group on the end. As discussed previously, it is possible that this structure is polymerizing when introduced into the melt and making a stronger reinforcement for the particles. At low levels of filler, this coupling agent is creating a stronger interface and strengthening the matrix, therefore, increasing the toughness. Although this was the only coupling agent to increase the toughness, several of the composites have increased tensile strength.

Larger errors were seen in elongation at break values for the composites that behave in a ductile manner. Bartczak et al.[37] explained the wide distribution of elongation at break values by a debonded particle mechanism creating voids in the matrix, where cracks are able to form and initially propagate stably away from the source. The chance of the propagating neck coming into contact with an imperfection was unpredictable and led to wide array of ultimate elongation values.

Tensile strength

Figure 11 shows composite tensile strengths versus volume percent for a selected few of the functional groups present on the coupling agents. Untreated boron nitride particles show an increase over neat HDPE but little effect on tensile strength with increasing volume percent of filler, an expected result when there are weak interactions between the filler and the matrix.[38] Surface treatment of the particles show an increase in tensile strength compared to the particles with no treatments. In particular, boron nitrides treated with silanes C, D, E, and F have

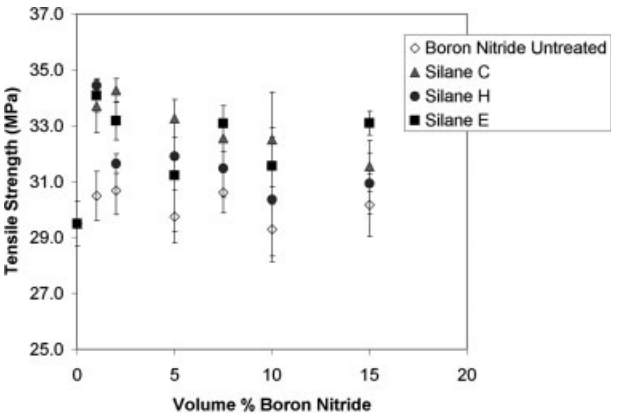

Figure 11 Tensile strength versus volume percent boron nitride for with silane coupling agents.

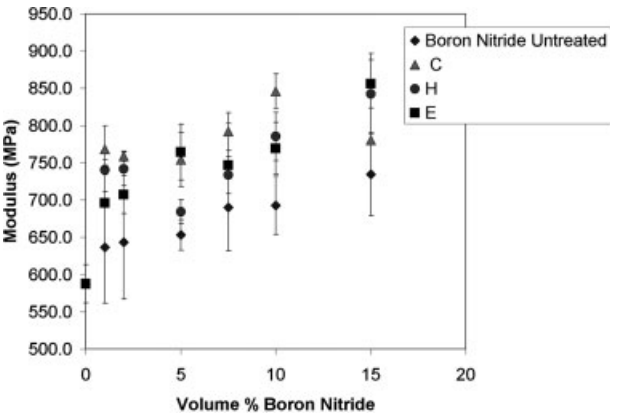

Figure 12 Young's modulus for BN composites treated with coupling agents.

significantly higher tensile strengths than the untreated control. Silanes G and H do not seem to affect the composite tensile strengths.

Samples C and E contain C=C bonds that could potentially undergo thermally initiated polymerization with themselves or defects on nearby polyethylene chain segments. Composites based on these functional groups all had higher tensile strengths than the untreated control. Sample F, synthesized with the short-chain polyethylene oxide, also had higher tensile strengths than the control. Samples G and H, based on an epoxide and a straight chain alkane functional groups, had improved tensile strengths at low filler volume fractions, and showed little improvement over the control at higher filler levels.

Parsons et al.[25] proposed a filler debonding mechanism to explain the decrease in tensile strength as the filler volume fraction increases in HDPE. When the stress at the interface exceeds its adhesive strength, the particles debond from the matrix. The debonded particles act as holes in the matrix causing stress in matrix ligaments to increase and resulting in the matrix yielding. As the volume fraction of filler increases, the number of holes caused by debonding particles at a given stress level increases, decreasing the tensile strength. Atikler et al.[31] also reported decreasing tensile strengths with increasing filler volume fractions when larger amounts of fillers are present (10 and 40 vol %) because of the particle debonding in fly ash/HDPE composites. In this study, at 1 vol % filler loading, all the silanes increase the tensile strength of the composite over the untreated control. The interface appears to be strengthened and the particles do not debond from the matrix as easily as the untreated powder.

Young's modulus

Young's modulus increases with the addition of the filler for neat BN composites. Figure 12 shows the tensile modulus values for the untreated particles compared to those treated with the coupling agents. All the treated fillers had modulus values greater than the control. Samples C and H had consistently higher moduli at low volume percent compared to other treatments. At higher particle loading all treated samples show an increase in modulus. At 15 vol % filler sample E has the highest modulus value. At high loading levels, particle–particle interactions may begin to affect the fracture mechanics. The filler controls the deformation of the polymer in the elastic zone. As the volume percent of filler increases less deformation of the polymer is seen and the Young modulus increases.[31]

Matrix-particle adhesion

Mechanical properties of composites are closely related to interfacial adhesion between the particles and the polymer matrix. Poor adhesion causes reduced load transfer and mechanical properties are adversely affected.[31] Coupling agents can improve adhesion between the particles and the matrix, causing the composite to fail due to shear yield and tearing rather than because voids are present. Intimate wetting contact must be made for surfaces to be adhered to reinforce the matrix.[23] Lazzeri et al.[30] found that coupling agents improved dispersion and also strongly increases in yield strength and modulus. Atikler et al.[31] was able to explain an increase in tensile strength due to better adhesion by using a silane coupling agent. Our results show an increase in modulus and tensile strength for those particles treated with a silane coupling agent. However, a decrease is seen in tensile strength when the volume of particles increases.

Interfacial adhesion is a critical factor in improving mechanical properties of composites. Mechanical strength is determined by two factors: compatibility between inorganic filler and polymer and the presence of cracks, voids, and fractures in the interphase. Silane coupling agents help to adhere the filler into

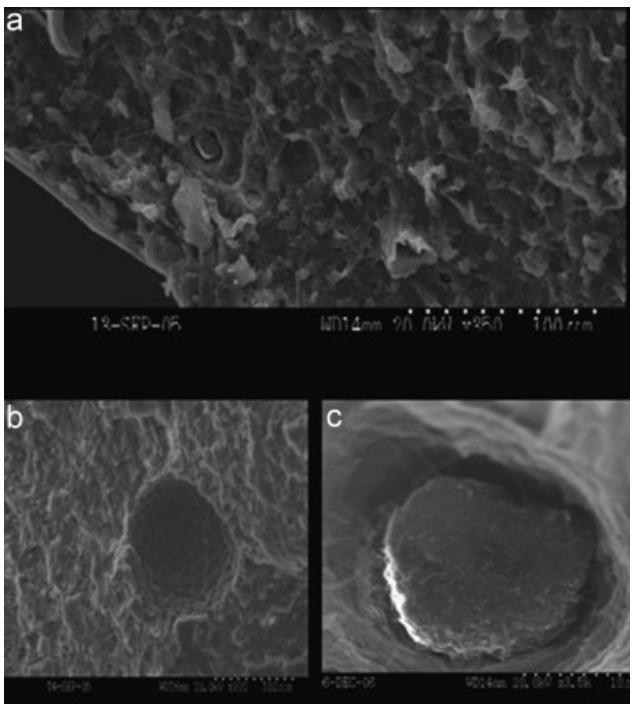

Figure 13 (a) SEM picture of fractured surface of untreated boron nitride powder showing, (b) particle debonded from matrix, and (c) particle still intact in the matrix.

the matrix and eliminate debonding from the matrix that leads to voids and premature fractures. Untreated fillers are more likely to pull out of the matrix under tensile stress than those that have had surface modifications.[31]

A critical debate exists about particles debonding from the polymer matrix during impact testing. There are a number of suggested mechanisms on how inorganic fillers affect impact,[30,37,38] and a complete analysis would require a separate study.

Matrix-particle morphology

Morphologies at fracture surfaces provide information about the failure mechanisms and adhesion between particles and the matrix. Figure 13(a) (calibration bar = 100 μm) shows the fracture surface of the control composite with untreated boron nitride powder. Figure 13(b,c) show specific particles on the fractured surface. Figure 13(b) shows a void from which a particle debonded during fracture; the interfacial adhesion was not very strong and there is an absence of microfibrils (which would demonstrate interfacial adhesion) on the void surface. Figure 13(c) shows a particle that is still intact in the matrix. The particle is surrounded by an air void, and there appears to be nothing attaching this particle into the polymer matrix. With no interfacial adhesion present, this composite failed by the particle acting as a void and not providing stress transfer from the matrix.

Figure 14 illustrates the fractured surfaces of Sample C with increasing volume percent filler. This coupling agent is shown because of the superior mechanical properties seen. A ductile fracture with low level of filler is shown in Figure 14(a) where the fibrils are elongated and aligned under tension. At a higher particle loading, 5 vol % in Figure 14(b), several particles can be seen on the fractured surface.

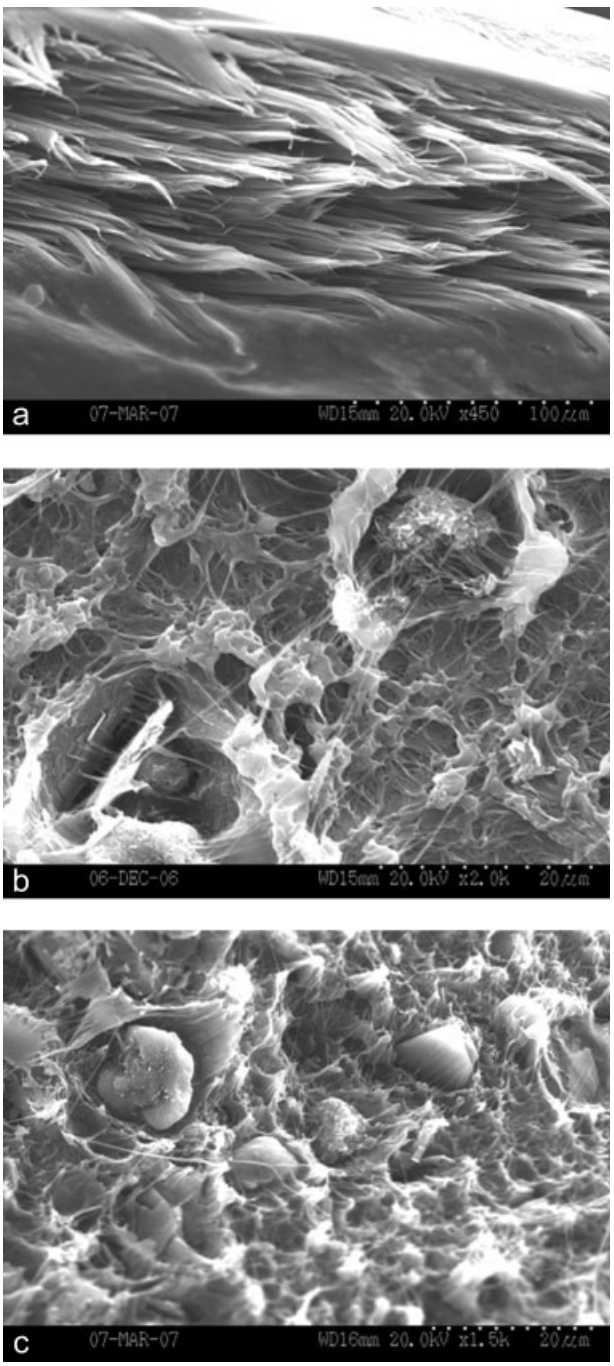

Figure 14 (a) 1 vol % of BN treated with styrylethyl trimethoxysilane; (b) 5 vol % BN treated with styrylethyl trimethoxysilane; and (c) 15 vol % BN treated with styrylethyl trimethoxysilane.

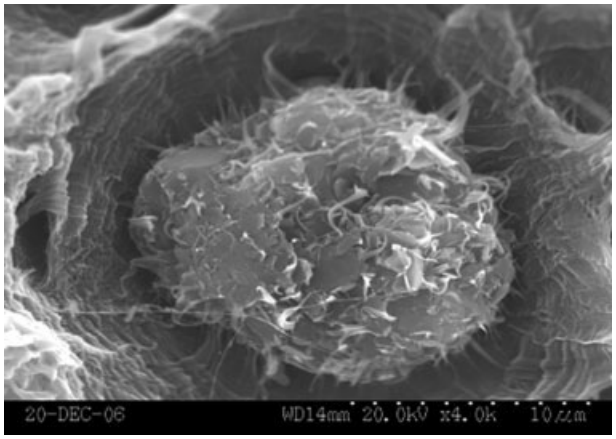

Figure 15 SEM picture of particle still in matrix on fractured surface treated with styrylethyl trimethoxysilane.

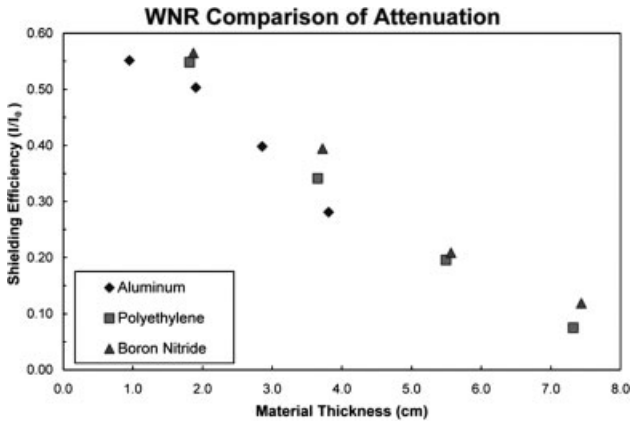

Figure 16 WNR comparison of attenuation results for aluminum, polyethylene, and PE/BN composites.

Figure 14(c) shows 15 vol % filler and the number of particles has increased compared to 5 vol % as expected. A closer look at a particle still in the matrix is shown in Figure 15. Microfibrils can clearly be seen between the particle and the matrix showing improved adhesion compared to the untreated particles. SEM micrographs show a transition from a ductile to brittle material between 7.5 and 10 vol % filler due to the increase in particles. In these images, the particles can still be seen in each of the holes present on the surface of the material. These particles did not debond from the matrix upon the composite fracturing. This coupling agent has allowed the particles to be clearly interlaced into the matrix of the polyethylene. The interface of the matrix and particle are connected consistent with the mechanical properties that were found. All of the coupling agents resulted in composites with similar SEM images. The interfacial adhesion was stronger between the particles and the matrix consistent with the increased mechanical properties found.

Neutron absorption results

The neutron and proton transmission fractions can be seen in Figures 16 and 17, respectively. Plotted on the *y* axis is the shielding efficiency, which is the ratio of the dose rate with the shielding material present to the dose rate with no shielding present. The faster the shielding efficiency goes to zero, the better the overall material is at attenuating the incident radiation. Plotted along the *x* axis is the thickness of the material. In the WNR neutron beam energies, polyethylene exhibits a better overall shielding efficiency than the boron nitride containing materials. Both polyethylene and boron nitride containing polyethylene exhibited similar shielding efficiencies to that of aluminum. In the WNR and upper atmosphere high energy neutron radiation environment, the polyethylene-based materials have the advantage of not producing long-lived radioactive progeny that could produce more radiation. The aluminum counterpart produced longer-lived progeny that yielded high-energy beta and photon radiation as a result of neutron captures.

In the high-energy proton shielding, the polyethylene compounds behaved similarly to one another. For the FNAL proton beam, the protons were at such a high energy that spallation could occur. The polyethylene-based materials actually caused more spallation products to enter the tank, causing a higher overall dose. Aluminum proved to be the better shielding material for high-energy protons. In the WNR beam, even though the polyethylene materials exhibited similar shielding capabilities, the pure polyethylene-based products were less effective than those that have the boron additives. The polyethylene containing boron nitride, however, stayed closer to unity than the pure polyethylene counterpart. For shield thickness less than 8 cm, the boron nitride containing polyethylene proved to be the better of the two composites. At these energies, the increasing thickness will increase the spallation ''spray'' and raise the over-

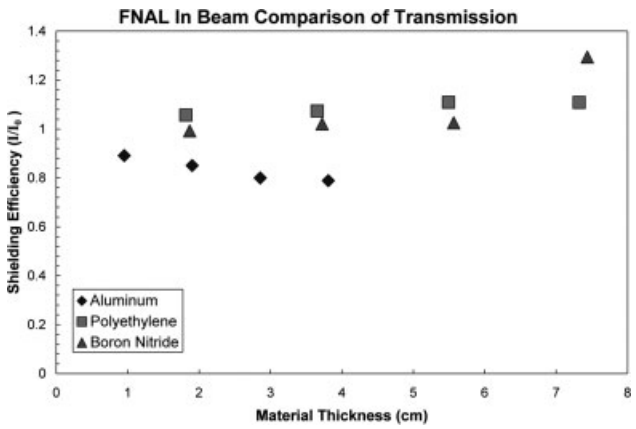

Figure 17 FNAL in beam comparison of transmission for aluminum, polyethylene, and PE/BN composites.

all dose. It should be noted that at 120 GeV, it takes several meters of solid steel to bring these energetic particles to rest.

CONCLUSIONS

The use of a hydrogen-rich polymer filled with low atomic mass filler could be useful in the future as a shielding material. The addition of boron does not offer much of an advantage until one reaches lower neutron energies. Boron nitride in polyethylene shows improved mechanical properties over that of neat polyethylene. Modifying the surface of the boron nitride particles shows even greater mechanical improvements over the untreated powders. The boron nitride composite shows tensile modulus values greater than the neat polymer. Functionalization of the powder surfaces increases this value even more. Addition of the boron nitride powder shows little effect on the tensile strength compared to the HDPE, but addition of the coupling agent increases the tensile strength greater than that for HDPE. The toughness of the composite is less than that of the neat polymer as expected due to the voids created by the particles. However at 1 vol %, the toughness was increased over the untreated powder. The adhesion of the particle into the polymer matrix is critical in improving the mechanical properties. From the SEM pictures, it is clear that surface modifications of the powder allow for better adhesion at the interface. An increase in mechanical properties was seen due to this improved property.

Based on the testing at various high energy neutron and proton facilities, it is recommended that the mechanical properties is to be further tested to determine which will be most effective as a shielding material. As these polyethylene composites are roughly 1/3 the density and have similar shielding abilities to the conventional aluminum counterpart, this material is a viable space radiation shielding material. In addition, the ability of the polyethylene-based materials to shield these radiation fields, and not produce long-lived, or high-energy gamma emitting progeny is of additional merit. Future investigation is being performed on that the material to be considered for a low energy neutron shielding material for shielding of neutron spectra in and around nuclear reactors.

References

1. Haffner, J. W. Radiation and Shielding in Space; Academic Press, 1967.
2. Kim, M. Y.; Thibeault, S. A.; Wilson, J. W.; Kiefer, R. L.; Orwoll, R. A. ACS Symposium Series 1996, 620, 350.
3. French, F. W. Journal of Spacecraft and Rockets 1966, 3, 1544.
4. Jakel, O. Z Med Phys 2004, 14, 267.
5. George, J. A. AIP Conference Proceedings 1992, 246, 130.
6. Spillantini, P. Nuclear Physics B, Proceedings Supplements 2000, 85, 3.
7. Curtis, S. B. Radioprotection 1993, 28, 179.
8. Simonsen, L. C.; Wilson, J. W.; Kim, M. H.; Cucinotta, F. A. Health Physics 2000, 79, 515.
9. Wilson, J. W.; Cucinotta, F. A.; Miller, J.; Shinn, J. L.; Thibeault, S. A.; Singleterry, R. C.; Simonsen, L. C.; Kim, M. H. Materials Research Society Symposium Proceedings 1999, 551, 3.
10. Zeitlin, C.; Guetersloh, S. B.; Heilbronn, L. H.; Miller, J. Nuclear Instruments and Methods in Physics Research B 2006, 252, 308.
11. Guetersloh, S.; Zeitlin, C.; Heilbronn, L.; Miller, J.; Komiyama, T.; Fukumura, A.; Iwata, Y.; Murakami, T.; Bhattacharya, M. Nuclear Instruments and Methods in Physics Research B 2006, 252, 319.
12. Ashton-Patton, M. M.; Hall, M. M.; Shelby, J. E. Journal of Non-Crystalline Solids 2006, 352, 615.
13. Clayton, L. M.; Gerasimov, T. G.; Cinke, M.; Meyyappan, M.; Harmon, J. P. Journal of Nanoscience and Nanotechnology 2006, 6, 2520.
14. Lin, Q.; Yang, B.; Li, J.; Meng, X.; Shen, J. Polymer 2000, 41, 8305.
15. Pavlenko, V. I.; Epifanovskii, I. S.; Lipkanskii, V. M.; Marakin, O. A. Perspektivnye Materialy 2003, 29.
16. Zhamu, A.; Zhong, W. H.; Hou, Y. P.; Stone, J. J. Proceedings of the American Society for Composites, Technical Conference 20th 2005, 45, 1.
17. Liu, L.; He, L.; Yang, C.; Zhang, W.; Jin, R.-G.; Zhang, L.-Q. Macromolecular Rapid Communications 2004, 25, 1197.
18. Ko, S. C.; Pugh, C. S.; Kiefer, R. L.; Orwoll, R. A. Materials Research Society Symposium Proceedings 1999, 551, 275.
19. Kraus, W. B.; Glasgow, M. B.; Kim, M. Y.; Olmeijer, D. L.; Kiefer, R. L.; Orwoll, R. A.; Thibeault, S. A. Polymer Preprints (American Chemical Society, Division of Polymer Chemistry) 1993, 34, 592.
20. Larrazabal, H. J.; Hrymak, A. N.; Vlachopoulos, J. Rheologica Acta 2006, 45, 705.
21. Sentmanat, M. L.; Muliawan, E. B.; Hatzikiriakos, S. G. Annual Technical Conference - Society of Plastics Engineers 63rd, 2005, 1097.
22. Muliawan, E. B.; Hatzikiriakos, S. G.; Sentmanat, M. International Polymer Processing 2005, 20, 60.
23. Sentmanat, M.; Hatzikiriakos, S. G. Rheologica Acta 2004, 43, 624.
24. Seth, M.; Hatzikiriakos, S. G.; Clere, T. M. Polymer Engineering and Science 2002, 42, 743.
25. Yip, F.; Diraddo, R.; Hatzikiriakos, S. G. Journal of Vinyl & Additive Technology 2000, 6, 196.
26. Parsons, E. M.; Boyce, M. C.; Parks, D. M.; Weinberg, M. Polymer 2005, 46, 2257.
27. Fu, Q.; Wang, G. Polymer International 1993, 30, 309.
28. Fu, Q.; Wang, G. Journal of Applied Polymer Science 1993, 49, 1985.
29. Fu, Q.; Wang, G.; Shen, J. Journal of Applied Polymer Science 1993, 49, 673.
30. Gonzalez, J.; Albano, C.; Ichazo, M.; Diaz, B. European Polymer Journal 2002, 38, 2465.
31. Lazzeri, A.; Zebarjad, S. M.; Pracella, M.; Cavalier, K.; Rosa, R. Polymer 2005, 46, 827.
32. Atikler, U.; Basalp, D.; Tihminlioglu, F. Journal of Applied Polymer Science 2006, 102, 4460.
33. Baraton, M. I.; Merle, T.; Quintard, P.; Lorenzelli, V. Langmuir 1993, 9, 1486.
34. Zhou, W.; Qi, S.; Li, H.; Shao, S. Thermochimica Acta 2007, 452, 36.
35. Ferenci, M. R. S.; Hertel, N. Radiation Protection Dosimetry 2003, 107, 213.
36. Bartczak, Z.; Argon, A. S.; Cohen, R. E.; Weinberg, M. Polymer 1999, 40, 2347.
37. Tanniru, M.; Yuan, Q.; Misra, R. D. K. Polymer 2006, 47, 2133.
38. Atikler, U.; Basalp, D.; Tihminlioglu, F. J. Appl. Polym. Sci. 2006, 102, 4460.